J Nanopart Res (2017) 19: 58
DOI 10.1007/s11051-017-3744-7

RESEARCH PAPER

The risk assessment of Gd_2O_3:Yb^{3+}/Er^{3+} nanocomposites as dual-modal nanoprobes for magnetic and fluorescence imaging

Long Huang · Xiumei Tian · Jun Liu · Cunjing Zheng · Fukang Xie · Li Li

Received: 28 October 2016 / Accepted: 4 January 2017 / Published online: 9 February 2017

Abstract Our group has synthesized Gd_2O_3:Yb^{3+}/Er^{3+} nanocomposites as magnetic/fluorescence imaging successfully in the previous study, which exhibit good uniformity and monodispersibility with a mean size of 7.4 nm. However, their systematic risk assessment remains unknown. In this article, the in vitro biocompatibility of the Gd_2O_3:Yb^{3+}/Er^{3+} was assessed on the basis of cell viability and apoptosis. In vivo immunotoxicity was evaluated by monitoring the product of reactive oxygen species (ROS), clusters of differentiation (CD) markers, and superoxide dismutase (SOD) in Balb/c mice. No significant differences were found in cell viability, apoptosis, and immunotoxicity between our Gd_2O_3:Yb^{3+}/Er^{3+} and gadodiamide which are used commonly in clinical. Few nanoprobes were localized in the phagosomes of the liver, heart, lung, spleen, kidney, brain, and tumor under the transmission electron microscopy (TEM) images. In addition, our products reveal good T_1-weighted contrast enhancement of xenografted murine tumor. Therefore, the above results may contribute to the effective application of Gd_2O_3:Yb^{3+}/Er^{3+} as molecular imaging contrast agents and dual-modal nanoprobes for cancer detection.

Keywords Nanocomposites · Biocompatibility · Immunotoxicity · Magnetic resonance imaging · Tissue targeted imaging · Health effects

Long Huang and Xiumei Tian have contributed equally to this work.

Electronic supplementary material The online version of this article (doi:10.1007/s11051-017-3744-7) contains supplementary material, which is available to authorized users.

L. Huang · C. Zheng · F. Xie (✉)
Department of Histology and Embryology, Zhongshan School of Medicine, Sun Yat-sen University, Guangzhou 510080, People's Republic of China
e-mail: frankxie2000@yahoo.com

X. Tian
Department of Biomedical Engineering, Guangzhou Medical University, Guangzhou 510182, People's Republic of China

J. Liu
School of Electronics and Information Technology, Guangdong Ocean University, Zhanjiang 524094, People's Republic of China

L. Li (✉)
State Key Laboratory of Oncology in South China, Imaging Diagnosis and Interventional Center, Sun Yat-sen University Cancer Center, Guangzhou 510060, People's Republic of China
e-mail: li2@mail.sysu.edu.cn

Introduction

Currently, the development of rare earth-based nanoparticles is attracting extensive interest for bioimaging applications. Among the multifarious imaging techniques, magnetic resonance imaging (MRI) is one of the most powerful and noninvasive diagnostic tools which can offer remarkable anatomical details for soft tissues (Liang et al. 2000). However, the high potential of false-positive signal usually brings about low sensitivity, long imaging time, and poor accuracy in traditional single modal MRI research (Caravan 2006). Although

fluorescence (FL) imaging can provide high sensitive, molecular level, and real-time imaging information, the low spatial resolution and poor tissue penetration depth prevent it from deep tissue imaging (Liu et al. 2011; Robinson et al., 2012; Ruedas-Rama et al. 2012; Liu et al. 2013). Consequently, as contrast agents, utility MR/FL nanoprobes are urgently needed to achieve accurate tumor diagnosis. However, due to their different shapes, small size, high surface-to volume ratios, positive surface charges and so on, they might do harm to human health potentially. Therefore, it is particularly important to evaluate the risk assessment of these materials.

In our previous research, Gd_2O_3:Yb^{3+}/Er^{3+} nanocomposites have been successfully synthesized as a potential dual-modality nanoprobe, but have not yet perform assessments of its toxicity in vitro and in vivo (Liu et al. 2016). Here, we systematically evaluated the toxicity of our nanocomposites including cell viability and apoptosis, serum SOD levels, reactive oxygen species (ROS) assays, and the cluster of differentiation (CD) markers. These studies are necessary to meet the needs of preclinical application.

Materials and experimental section

Synthesis of the nanomaterials

Laser ablation of Gd_2O_3 in liquid has been shown in our previous work (Liu et al. 2016). The ablated samples were collected by centrifuge to exclude large materials prior to further applications in vitro and in vivo.

Cytotoxicity assay

The human nasopharyngeal carcinoma CNE-2 cells and immortalized nasopharyngeal epithelial NP69 cells were cultured with PRMI-1640 media (Gibco, Grand Island, NY, USA) with 10% fetal bovine serum (FBS, Gibco, Grand Island, NY, USA) and keratinocyte-serum free medium (K-SFM, Gibco, USA) with epidermal growth factor and bovine pituitary extract in 96 wells plates, respectively. Cells were incubated with different concentrations of Gd_2O_3:Yb^{3+}/Er^{3+} (1 × phosphate-buffered saline (PBS) pH 7.4, 100 nM, 1 μM, and 10 μM) and gadodiamide (10 μM) during their logarithmic growth period. Treatment with culture media and 5% dimethyl sulfoxide (DMSO) was used as the negative control and the positive control, respectively. All groups were cultured in cell incubator (5% CO_2, 37 °C) for 24 h before being measured by Cell Counting Kit-8 (CCK-8) (Dojindo, Japan) according to the manufacturer's instructions. Each well was incubated with 10 μL of CCK-8 solution in incubator for 4 h. Absorbance at 450 nm was measured using a microplate reader (Bio-Rad, Japan).

Apoptosis assay

CNE-2 cells and NP69 cells were incubated with PBS (negative control), lipopolysaccharides (LPS; positive control), gadodiamide (10 μM), and the Gd_2O_3:Yb^{3+}/Er^{3+} (10 μM) in 6-well plates for 24 h. Cells were collected and washed twice with cold PBS by gentle shaking. Then, we measured with Annexin ∨ − FITC Apoptosis Analysis Kit (Tianjin Sungene Biotech Co., Ltd) according to the provided instructions. Finally, the samples were analyzed on a FACScan (USA).

In vivo immunotoxicity of the Gd_2O_3:Yb^{3+}/Er^{3+}

All animal experiments in this paper were purchased from the Animal Experiment Centre of the Medical College, Sun Yat-Sen University (People's Republic of China). Twenty male Balb/c mice, 5–6 weeks old, were housed in temperature-controlled, light-cycle room in animal facilities, with unlimited food and water. Balb/c nude mice (4–5 weeks old, weight of 16 ± 2 g) were maintained in a pathogen-free animal facility. The study protocol was approved by the Care and Use of Laboratory Animals of Sun Yat-sen University (Permit Numbers: SCXK (Guangdong) 2011–0029). We followed the guidelines of the Care and Use of Laboratory Animals of Sun Yat-sen University during the study.

Twenty male Balb/c mice, 5–6 weeks old, were divided into four groups at random and injected via tail vein: (a) PBS (100 μL; negative control), (b) LPS (5 mg/kg), (c) gadodiamide (15 μmol/kg), and (d) Gd_2O_3:Yb^{3+}/Er^{3+} (15 μmol/kg). Samples were gained after 7 days post-injection and measured by flow cytometry.

Expression levels of superoxide dismutase (SOD) in serum

Peripheral blood from the ophthalmic vein was added to 1.5 mL Eppendorf tubes and kept for 45 min. Samples were centrifuged at 3000 g for 10 min at 4 °C. The supernatant was transferred into new tubes and SOD levels

were measured with ELISA kits (RayBiotech, Inc., Guangzhou, China) according to the provided instructions.

ROS assay on peripheral blood neutrophils

Peripheral blood from the tail vein (20 μL) was added to the tube with heparin sodium (4 μL). Erythrocytes were lysed by red blood cell lysis buffer (pH 7.4) in the dark for 2 min. Then, we added PBS (2 mL) and centrifuged the samples at 1200 g for 5 min at 4 °C. 2′, 7′-Dichlorodihydrofluorescein diacetate (H2DCFDA) was added to the samples at a final concentration of 5 μM. Cells were mixed thoroughly in the dark for 20 min and PBS (400 μL) was added.

Expression of representative CD markers in peripheral blood

Peripheral blood (20 μL) from the vena ophthalmica was collected into the tube containing heparin sodium (4 μL). The erythrocytes were lysed in the dark for 2 min. Then, we added 2 mL PBS and centrifuged at 1200 g for 5 min. Cells were stained in the dark for 30 min with anti-mouse CD69-FITC, anti-mouse CD3-PE, anti-mouse CD206-PE, anti-mouse CD11b-PE, anti-mouse CD25-FITC, anti-mouse CD71-FITC, and anti-mouse F4/80 antigen APC.

MRI in vivo

Balb/c nude mice (4–5 weeks old, weight of 16 ± 2 g) were subcutaneously injected with CNE-2 cells (5×10^6 in 100 μL PBS). Ten days after CNE-2 cell inoculation, mice with xenografted tumors of 6 mm^3 were induced with anesthesia by intraperitoneal injection of 1% mebumalnatrium (10 μL per gram bodyweight), then injected with Gd_2O_3:Yb^{3+}/Er^{3+} (15 μmol/kg) via the tail vein and scanned with a 3.0-T MRI system (Siemens Medical Solutions, Erlangen, Germany) using a 3-in. diameter surface coil constructed specifically for small animals. T1-weighted images were obtained at 0, 10, 20, 30, 60, and 100 min after intravenous administration of the Gd_2O_3:Yb^{3+}/Er^{3+} in the axial orientations.

Statistical analysis

All data are expressed as mean ± standard deviation (SD). Statistical analysis was performed by one-way ANOVA and one-sample t test by using the Origin 8.0 software. Data were considered significant when $p < 0.05$.

Results and discussion

Biocompatibility of Gd_2O_3:Yb^{3+}/Er^{3+} nanocomposites in vitro

The viability of the human nasopharyngeal carcinoma CNE-2 cells and immortalized nasopharyngeal epithelial NP69 cells were evaluated by cytotoxicity assay. Fifty percent inhibitory concentration of NP69 cells and CNE-2 cells are 13 mM and 194 μM, respectively. The Gd_2O_3:Yb^{3+}/Er^{3+} nanocomposites did not significantly affect the viability of two kinds of cells after incubation for 24 h (Fig.1a). In addition, apoptosis of cells relates to risk assessment in vitro (Tamura et al. 1995). Hence, we studied the apoptosis of CNE-2 and NP69 cells after co-incubation with Gd_2O_3:Yb^{3+}/Er^{3+} nanocomposites for 24 h. There is no significant difference between gadodiamide and the Gd_2O_3:Yb^{3+}/Er^{3+} (Fig.1b). Therefore, the results of the in vitro biocompatibility showed our nanocomposites are suitable for in vivo study.

Immunotoxicity of Gd_2O_3:Yb^{3+}/Er^{3+} nanocomposites in vivo

Although the Gd_2O_3:Yb^{3+}/Er^{3+} nanocomposites displayed promising biocompatibility in vitro, it is also vital to investigate the immune response in vivo. Superoxide dismutase (SOD) is a factor of primary importance in enabling organisms to survive the challenge presented by the reactive intermediate species resulting from the univalent resulting from the univalent reduction of molecular oxygen (McCord JM et al. 2014). As shown in Fig.2a, the SOD level of the Gd_2O_3:Yb^{3+}/Er^{3+} group was slightly increased comparing to the gadodiamide group. However, no significant difference was seen between the negative control group and the Gd_2O_3:Yb^{3+}/Er^{3+} group. Then, we evaluated the ROS of neutrophil in the peripheral blood since ROS takes part in immune conductive and triggers either immunosuppression or the eradication of pathogens during tissue restoration (Yang et al.2013). After 7 days injection, the ROS levels of the Gd_2O_3:Yb^{3+}/Er^{3+} group were decreased compared to the gadodiamide group (Fig.2b). As an immune mediator, ROS is relative to adaptive and the host innate immune response (Gaddis et al.2009; Kim et al.2012). Thus, we further studied the expression levels

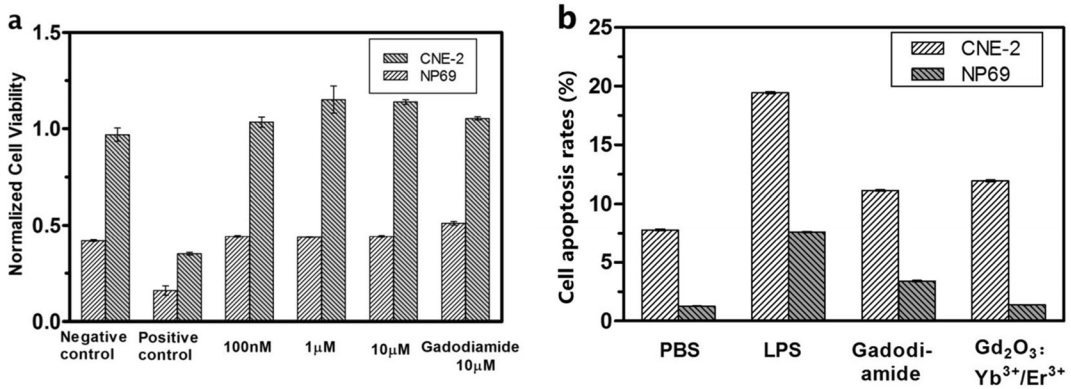

Fig. 1 In vitro biocompatibility of the Gd_2O_3:Yb^{3+}/Er^{3+} nanocomposites. **a** Cell viability of CNE-2 and NP69 cells incubated with different concentrations of Gd_2O_3:Yb^{3+}/Er^{3+} (100 nM, 1 μM, and 10 μM) at 24 h. **b** Apoptosis rates of CNE-2 and NP69 cells were analyzed by flow cytometry 24 h after incubation of PBS, LPS, gadodiamide (10 μM), and the Gd_2O_3:Yb^{3+}/Er^{3+} (10 μM). Samples were stained by Annexin ∨ and PI

of CD markers in peripheral blood. CD69 is an early antigen of T lymphocyte activation (Sancho et al.2005). CD71 and CD25 are surface markers in activated T cells (Samarasinghe et al. 2010). CD11b is expressed on immature macrophages and blood monocytes (Roca et al. 2009); CD206 is mainly present on tissue macrophages (Akbarshahi et al.2012). Consequently, their expression levels are an important parameter in assessing lymphocyte, activated T cells, and monocytes/macrophages. The results showed no obvious difference between the Gd_2O_3: Yb^{3+}/Er^{3+} group and the gadodiamide group (Fig.2c). In general, our nanocomposites may have few effects on the immune system and indicate a satisfactory immunotoxicity.

Pathological biopsy assay of the Gd_2O_3:Yb^{3+}/Er^{3+} nanocomposites

The pathological analysis was conducted on major organs containing lung, brain, liver, spleen, kidney, heart, and CNE-2 xenograft tumor 24 h after Gd_2O_3:Yb^{3+}/Er^{3+} injection (15 μmol/kg) (Fig.3). Samples were fixed with 4% paraformaldehyde, embedded in paraffin, sectioned, and stained with hematoxylin and eosin. As shown in Fig.3, there were no abnormal changes in any histological sections, which demonstrated that the cellular integrity and tissue morphology were not affected by the nanocomposites. Hence, it is significant for in vivo immunotoxity studies to assess the possible health hazard.

Biodistribution of the Gd_2O_3:Yb^{3+}/Er^{3+} nanocomposites at the subcellular level

Evaluating the biocompatibility of nano-based biomedicine includes the assessment of its biodistribution (Dobrovolskaia et al. 2008). Here, we used TEM to further visualize the nanopartical biodistribution at the subcellar level. Sections of the brain, kidney, liver, heart, lung, spleen, and CNE-2 xenograft tumor were observed

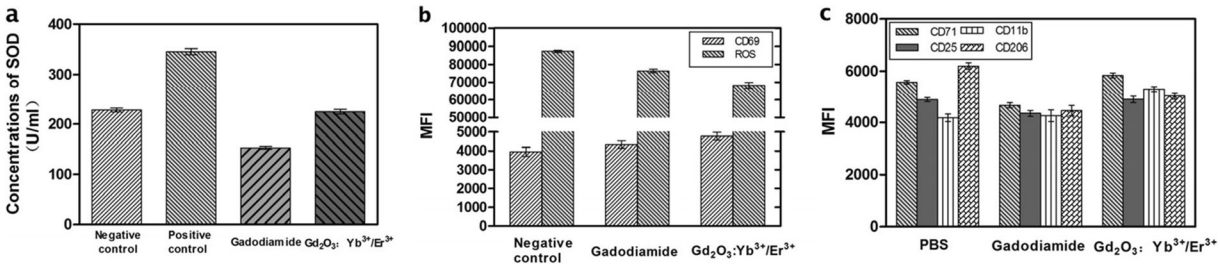

Fig. 2 Toxicity on immunity was measured by flow cytometry at 7 days after injection in Balb/c mice (15μml/kg, mean ± SD, $n = 5$). **a** Concentrations of SOD in the serum. **b** Expression levels of CD69 in the lymphocyte cells of peripheral blood and ROS of neutrophils in peripheral blood, respectively. **c** The expression levels of CD71, CD25, CD11b, and CD206 in monocytes/macrophages of peripheral blood, respectively

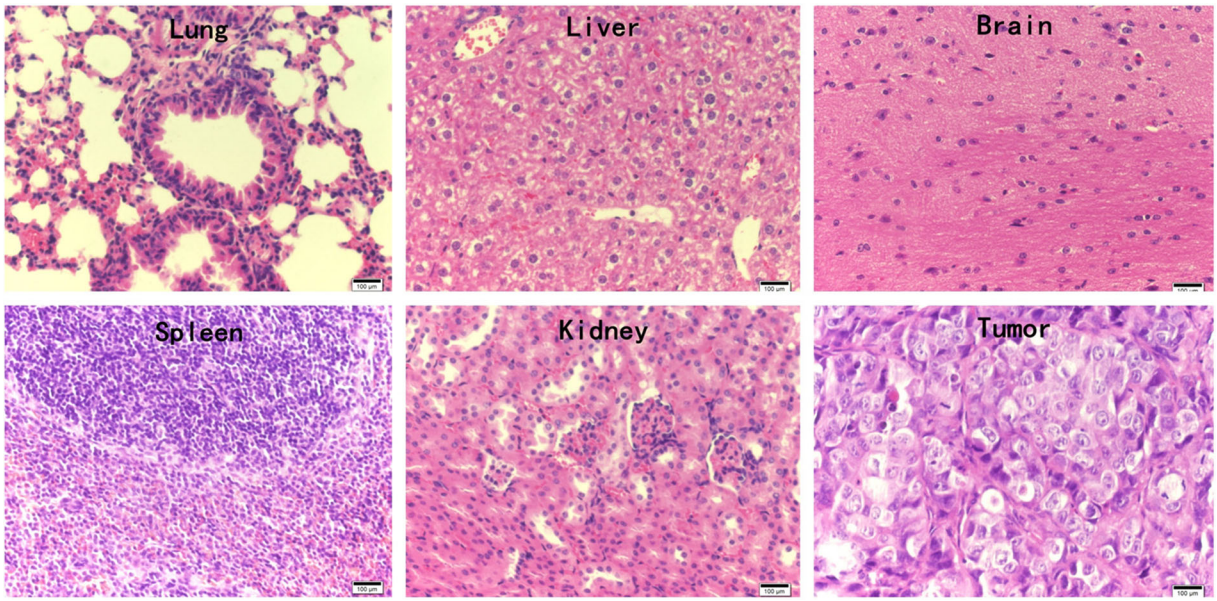

Fig. 3 Pathological biopsy assay of the Gd_2O_3:Yb^{3+}/Er^{3+} nanocomposites. Tissues were collected 24 h after Gd_2O_3:Yb^{3+}/Er^{3+} nanocomposites injection (15 μmol/kg) and stained with hematoxylin and eosin

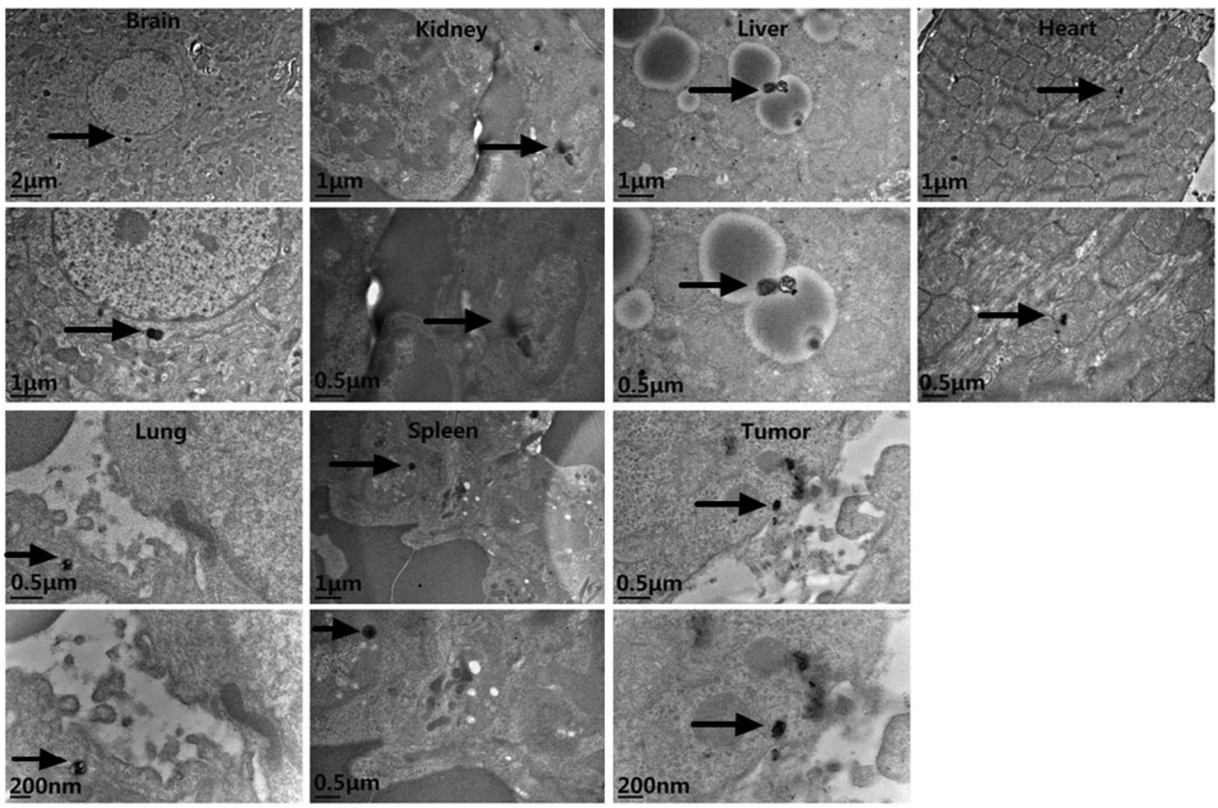

Fig. 4 TEM imaging of the Gd_2O_3:Yb^{3+}/Er^{3+} nanocomposites. Tissues were collected 4 h after Gd_2O_3:Yb^{3+}/Er^{3+} nanocomposites injection (*black arrow*; 15 μmol/kg)

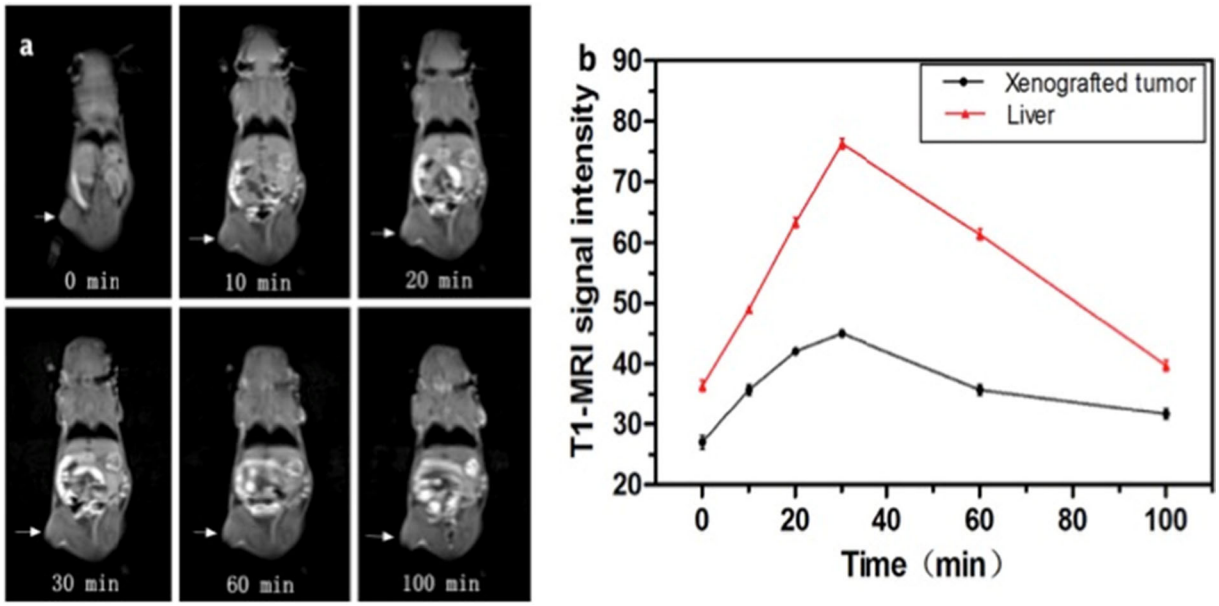

Fig. 5 Representative dynamic contrast-enhanced T1-weightd MR images of CNE-2 xenograft tumor after intravenous administration of the Gd_2O_3:Yb^{3+}/Er^{3+} nanocomposites (15 μmol/kg). **a** Subcutaneous xenograft tumor (*white arrow*) in mice at 0, 10, 20, 30, 60, and 100 min after injection of the nanoprobe. **b** The dynamic enhancement curve of xenografted tumor and normal liver

4 h after injection with the Gd_2O_3:Yb^{3+}/Er^{3+} nanocomposites (Fig. 4). A few nanocomposites were distributed in the cytoplasm of epithelial cells in the lung, heart, tumor tissue, and in the lysosomes of macrophages in the kidney, spleen, and liver. Meanwhile, a small amount of nanocomposites were found in the brain by infiltrating through the blood-brain barrier. These suggest that our nanocomposites were decentralized inside the phagosomes of the main organs and exhibited aggregation except the liver. Hence, the nanocomposites did slightly damage the microstructure or ultrastructure of the cells, which may induce the toxic effects in vivo including the oxidative stress and immunotoxicity.

In vivo MRI

After injection with Gd_2O_3:Yb^{3+}/Er^{3+} nanocomposites via the tail vein, we obtained T_1-weighted images in the axial orientations at 0, 10, 20, 30, 60, and 100 min (Fig. 5). The xenografted tumor could be successfully imaged in a short time and showed a high contrast enhancement at 30 min post-injection, which indicated that our nanocomposites might be a good MRI contrast agent for biomedical applications.

Conclusion

In summary, our nanocomposites have minimal cytotoxicity, satisfactory biocompatibility in vitro, and weak immunotoxicity in vivo. In addition, few nanoprobes were localized in the phagosomes of main organs under the TEM images, which shows the nanoparticles did slightly damage the microstructure or ultrastructure of the cells. Furthermore, Gd_2O_3:Yb^{3+}/Er^{3+} nanoparticles showed contrast enhancement for MR imaging and hence could be considered as an ideal diagnostic probe for potential application in clinical research procedures and disease diagnosis. Thus, it can be seen that evaluating the biocompatibility of rare earth-based nanomaterials is very important.

Acknowledgements This work was supported by the National Basic Research Program of China (2014CB931700), the National Natural Science Foundation of China (Grant Nos.81471787, 61471401, 81471711, 81271622, and 11274394), the National Science Foundation for Young Scholars of China (Grant No. 81401462), Natural Science Foundation of Guangdong, China (No.2014A030311036), and State Key Laboratory of Optoelectronic Materials and Technologies (Sun Yat-Sen Unversity) (No.OEMT-2015-KF-03).

Compliance with ethical standards

Conflict of interest The authors report no conflicts of interest.

References

Akbarshahi H, Menzel M, Posaric BM, Rosendahl A, Andersson R (2012) Enrichment of murine $CD68^+$ $CCR2^+$ and $CD68^+CD206^+$lung macrophages in acute pancreatitis-associated acute lung injury. PLoS One 7:e42654

Caravan P (2006) Strategies for increasing the sensitivity of gadolinium based MRI contrast agents. ChemSocRev 35:512–523

Dobrovolskaia MA, Aggarwal P, Hall JB, Mcneil SE (2008) Interaction with the immune system and its potential effects on nanoparticle biodistribution. Mol Pharm 5:487–495

Gaddis DE, Michalek SM, Katz J (2009) Requirement of TLR4 and CD14 in dendritic cell activation by hemagglutinin B from Porphyromonas gingivalis. Mol Immunol 46:2493–2504

Kim HW, Cho SI, Bae S, Kim H, Kim Y, Hwang YI, Kang JS, Lee WJ (2012) Vitamin C up-regulates expression of CD80, CD86 and MHC Class II on dendritic cell line, DC-1 via the activation of p38 MAPK. Immune Netw 12(6):277–283

Liang ZP, Lauterbur PC (2000) Principles of magnetic resonance imaging:a signal processing perpective. Spie Optical Engineering 50(3):272–286

Liu Y, Ai K, Yuan Q, Lu L (2011) Fluorescence-enhanced gadolinium-doped zinc oxide quantum dots for magnetic resonance and fluorescence imaging. Biomaterials 32(4):1185–1192

Liu Z, Pu F, Huang S, Yuan Q, Ren J, Qu X (2013) Long-circulating Gd_2O_3:Yb^{3+}/Er^{3+} up-conversion nanoprobes as high-performance contrast agents for multi-modality imaging. Biomaterials 34(6):1712–1721

Liu J, Huang L, Tian XM, Shan YZ, Xie FK, Chen DH, Li L (2016) Magnetic and fluorescent Gd_2O_3:Yb^{3+}/ln^{3+} nanoparticles for simultaneous upconversion luminescence/MR dual modal imaging and NIR-induced photodynamic therapy. Int J Nanomedicine 12:1–14

McCord JM, Fridovich I (2014) Superoxide dismutases: you've come a long way, baby. Antioxid Redox Signal 20(10):1548–1549

Robinson JT, Hong G, Liang Y, Zhang B, Yaghi OK, Dai H (2012) In vivo fluorescence imaging in the second near-infrared window with long circulating carbon nanotubes capable of ultrahigh tumor uptake. J Am Chem Soc 134(25):10664–10669

Roca H, Varsos ZS, Sud S, Craig MJ, Ying C, Pienta KJ (2009) CCL2 and interleukin-6 promote survival of human $CD11b^+$ peripheral blood mononuclear cells and induce M2-type macrophage polarization. J Biol Chem 284:34342–34354

Ruedas-Rama MJ, Walters JD, Orte A, Hall EA (2012) Fluorescent nanoparticles for intracellular sensing: a review. Anal Chim Acta 751:1–23

Samarasinghe S, Mancao C, Pule M, Nawroly N, Karlsson H, Brewin J, Openshaw P, Gaspar HB, Veys P, Amrolia PJ (2010) Functional characterization of alloreactive T cells identifies CD25 and CD71 as optimal targets for a clinically applicable allodepletion strategy. Blood 115:396–407

Sancho D, Gómez M, Sánchez-Madrid F (2005) CD69 is an immunoregulatory molecule induced following activation. Trends Immunol 26:136–140

Tamura T, Ishihara M, Lamphier MS, Tanaka N, Oishi I, Aizawa S, Matsuyama T, Mak TW, Taki S, Taniguchi T (1995) An IRF-1-dependent pathway of DNA damage-induced apoptosis in mitogen-activated T lymphocytes. Nature 376:596–599

Yang Y, Bazhin AV, Werner J, Karakhanova S (2013) Reactive oxygen species in the immune system. IntRevImmunol 32:249–270